Universal Journal of Public Health 13(2): 456-470, 2025 http://www.hrpub.org
DOI: 10.13189/ujph.2025.130217

Spatial Autocorrelation Analysis of Infectious Disease Incidence Rates at State and District Level Using Supra-Adjacency Weights Matrix

Piau Phang[1,*], Saira Aslam[1], Jane Labadin[1], Vivek Jason Jayaraj[2]

[1]Faculty of Computer Science and Information Technology, Universiti Malaysia Sarawak, Malaysia
[2]Digital Health Division (Analytics & Informatics), Ministry of Health Malaysia, Malaysia

Received December 10, 2024; Revised February 10, 2025; Accepted March 17, 2025

Cite This Paper in the Following Citation Styles

(a): *[1] Piau Phang, Saira Aslam, Jane Labadin, Vivek Jason Jayaraj , "Spatial Autocorrelation Analysis of Infectious Disease Incidence Rates at State and District Level Using Supra-Adjacency Weights Matrix," Universal Journal of Public Health, Vol. 13, No. 2, pp. 456 - 470, 2025. DOI: 10.13189/ujph.2025.130217.*

(b): *Piau Phang, Saira Aslam, Jane Labadin, Vivek Jason Jayaraj (2025). Spatial Autocorrelation Analysis of Infectious Disease Incidence Rates at State and District Level Using Supra-Adjacency Weights Matrix. Universal Journal of Public Health, 13(2), 456 - 470. DOI: 10.13189/ujph.2025.130217.*

Abstract The spatiotemporal correlation in disease incidence rates resulting from the spatial arrangement of neighboring geographical units is often conceptualized through constructing contiguity-based spatial weights. However, these weights specifications are not meant for capturing the spatial relationships across multiple spatial scales and disjoint spatial units. Modifications to existing spatial weights specifications are highly required. Hence, this study used supra-adjacency matrix in network science to analyze the spatial autocorrelation of COVID-19 incidence rates at Sarawak's district and Malaysia's state levels. Flight routes between these regions were embedded as spatial interaction submatrix to represent their inter-layer adjacency. Segmentation of data based on respective Sarawak's and Malaysia's daily cases was conducted to investigate the consistency in the spatial autocorrelation and the type of local clustering. When global spatial autocorrelations at state level were high, both the Sarawak districts' and Malaysia states' incidence rates became more spatially related with the inclusion of spatial interaction. Several districts, including Sibu, in Sarawak were now classified as high-high cluster with supra-adjacency weights. These high-high clusters can only be discovered with second-order contiguity weights in previous literature. The numbers of significant spatial clusters and outliers in district level were substantially greater than its state-level counterpart. This research provides evidence on how spatial dependencies of disease incidence rates between two spatial aggregation levels and geographically disjoint regions can be quantified using supra-adjacency matrix for disease surveillance. Capturing inter-layer spatial dependencies allows for more targeted interventions such as optimizing vaccine distribution and planning mobility restrictions during pandemics.

Keywords Spatial Autocorrelation, Contiguity Weights, Supra-Adjacency Matrix, COVID-19 Incidence Rates

1. Introduction

Spatiotemporal analysis of infectious disease spread is pivotal and one of the earlier focuses in understanding the epidemiologic trends of coronavirus disease 2019 (COVID-19) [1,2]. A variety of spatial statistics techniques and geographical information system tools are being utilized in exploring the spatial pattern of the pandemic [3,4]. Spatial autocorrelation analysis is widely conducted to examine the degree of similarity between the daily confirmed case numbers over different geographical units and spatial aggregation levels, ranging from country [5], province [6], district [7], to neighborhoods in a city [8]. Unlike conventional compartmental models that assume homogeneous mixing in the host population [9,10], the georeferenced observations in spatiotemporal models are generally not independent of one another [11]. The spatial dependence of the attribute of interest between geographical units is commonly conceptualized by specifying spatial weights, which measure the influence of a geographical unit to another.

However, the spatial weight coefficients specification is a non-trivial problem [12]. There is no a concise theory for finding the true spatial weights matrix [13]. It is often reliant on the use of prior information and experience [14]. For simplicity's sake, a great majority of works of literature in spatiotemporal analysis of aggregated data of COVID-19 case number rely on the first-order contiguity-based spatial weights matrix in quantifying the spatial relations of the disease transmission phenomena (see for instance [15,16]). In contiguity matrices, two geographical units are considered as neighbors if they share a common border. Besides, distance-based spatial weights, which assign greater weight to nearby regions compared to distant regions via inverse distance matrix, are also commonly used, particularly for location point data. These geographical proximity-based spatial weights matrices, despite promising to comprehend the spatial dependencies between geographical units, the weights generated with such definitions may be controversial. For instance, small regions often have less number of border regions [17]. Depending on the nature of the process under study, two geographical units which are close geographically but separated by other factors (such as lack of accessibilities or opportunities) may not necessarily be more related than distant geographical units [18] or be considered as near neighbors [19]. Moreover, such concepts of contiguity and distance often cannot depict the realistic human mobility across geographical units [14].

Apart from contiguity- and distance-based spatial weights matrices, other spatial weights can also be defined by specifying spatial interaction [20] and covariates [19] of geographical units under observation. Interaction-based spatial weights are useful for incorporating flow of people between areas while covariate-based for socio-demographical factors. All these variants and their hybrid weights specifications were compared for spatiotemporal model fitting on COVID-19 data over small areas located in Valencia, Spain [21]. They found that the classical first-order contiguity and the inverse distance matrix were still the most suitable and performed better than those of covariate-based or hybrid type. A composite of contiguity and inverse distance spatial weight matrix gave greater autocorrelation of daily confirmed numbers for 14 selected countries in May 2020 than applying contiguity or distance-based weights alone [22]. Moreover, Belvis and co-workers [23] claimed that incorporating adjacency based on mobility flow did not improve the spatial autocorrelation values across five waves of COVID-19 in Catalonia, Spain, but contiguity criteria remained yielding higher autocorrelation. Despite various alternative spatial weights specifications are being employed, these findings suggest that contiguity-based spatial weights can provide valuable insights into the underlying spatial processes of COVID-19 disease transmission. Also, there remains a lack of studies on how these spatial weights can be useful for comprehending the spatial dependencies between different spatial aggregation levels.

The spatiotemporal clustering patterns of the pandemic at district level of Malaysia were also investigated using first-order contiguity-based spatial weights matrix [24,25]. The latter literature went further by considering the neighbors of neighbor through a second-order spatial contiguity and found that higher order contiguity could detect more visible patterns of spatial clusters and outliers for the co-evolution of COVID-19 daily confirmed cases in Sarawak. However, the study [25] only focused on districts in Sarawak without relating to the pandemic evolution in other states in Malaysia. As the largest state in Malaysia by land size and situated in East Malaysia, which is linked by road to Sabah but primarily by air transport to the Peninsular Malaysia, contiguity-based spatial weights fail to quantify the spatial relation between Sarawak's districts and other states in Peninsular Malaysia as they are geographically disjoint. Therefore, a clear gap in literature exists in specifying the spatial weights of geographical units across disjointed regions.

Hence, we proposed a novel supra-adjacency type of spatial weights matrix to specify the spatial dependence of two spatial aggregation levels, namely state and district, which are also geographically disjointed, in this study. Supra-adjacency matrix has a block-diagonal structure where its interior corresponds to intra-layer connections, and an off-block-diagonal structure containing the inter-layer connections. It serves as a fundamental representation for multilayer networks [26] such that multiple subsystems and layers of connectivity can be reckoned. Empirical studies of multilayer networks in various domains have existed for more than a decade (see [27] and the references therein), along with the prediction of COVID-19 infections [28].

This study contributes to the existing literature on the spatiotemporal analysis of epidemiological data by conceptualizing both spatial contiguity weights and spatial interaction weights into supra-adjacency matrix. The novelty of this work lies in its exploration of the spatial autocorrelation intensity for two spatial aggregation levels of disease incidence rates in supra-adjacency setting. The effect of different temporal segmentations on global and local spatial autocorrelation throughout the study period was also investigated. Furthermore, we included a schematic representation of supra-adjacency matrix and several toy example calculations to comprehend the basic terminologies in spatial statistics to readers, especially for public health officials who may not be familiar with spatiotemporal analysis. This research provides empirical evidence on how spatial dependencies between different spatial aggregation levels and across geographically disjoint regions can be quantified on top of purely spatial proximity for disease surveillance and response in preparation for next pandemic.

2. Materials and Methods

2.1. Data Source and Study Area

This study extended the spatial autocorrelation analysis of COVID-19 incidence rates in 40 districts in the state of Sarawak (Fig. 1(a)) by considering Malaysia's state-level (Fig. 1(b)) incidence rates through a supra-adjacency spatial weights specification. The district-wise daily COVID-19 confirmed cases data throughout 2021 were extracted from the daily press statements published by the Sarawak Disaster Management Committee (SDMC). Since the onset of pandemic, SDMC has been managing the COVID-19 situations within the state and disseminating the information on various control measures, including travel restrictions across districts and states, to general public in Sarawak [29]. The year 2021 was chosen as the study period to coincide with the first three peaks in COVID-19 infections in Sarawak. Also, throughout this study period, the confirmed cases were mainly registered on a day-to-day basis by nearest local health authority after receiving the infected patients' polymerase chain reaction test results, as opposed to self-testing using rapid antigen test kits and self-reporting cases through a contact tracing application (CTA) in the subsequent years. The former approach is more reliable in capturing the exact physical location of the infected patients, while the latter approach relies heavily on the CTA users' permanent address which may be different substantially from their exact geographical location.

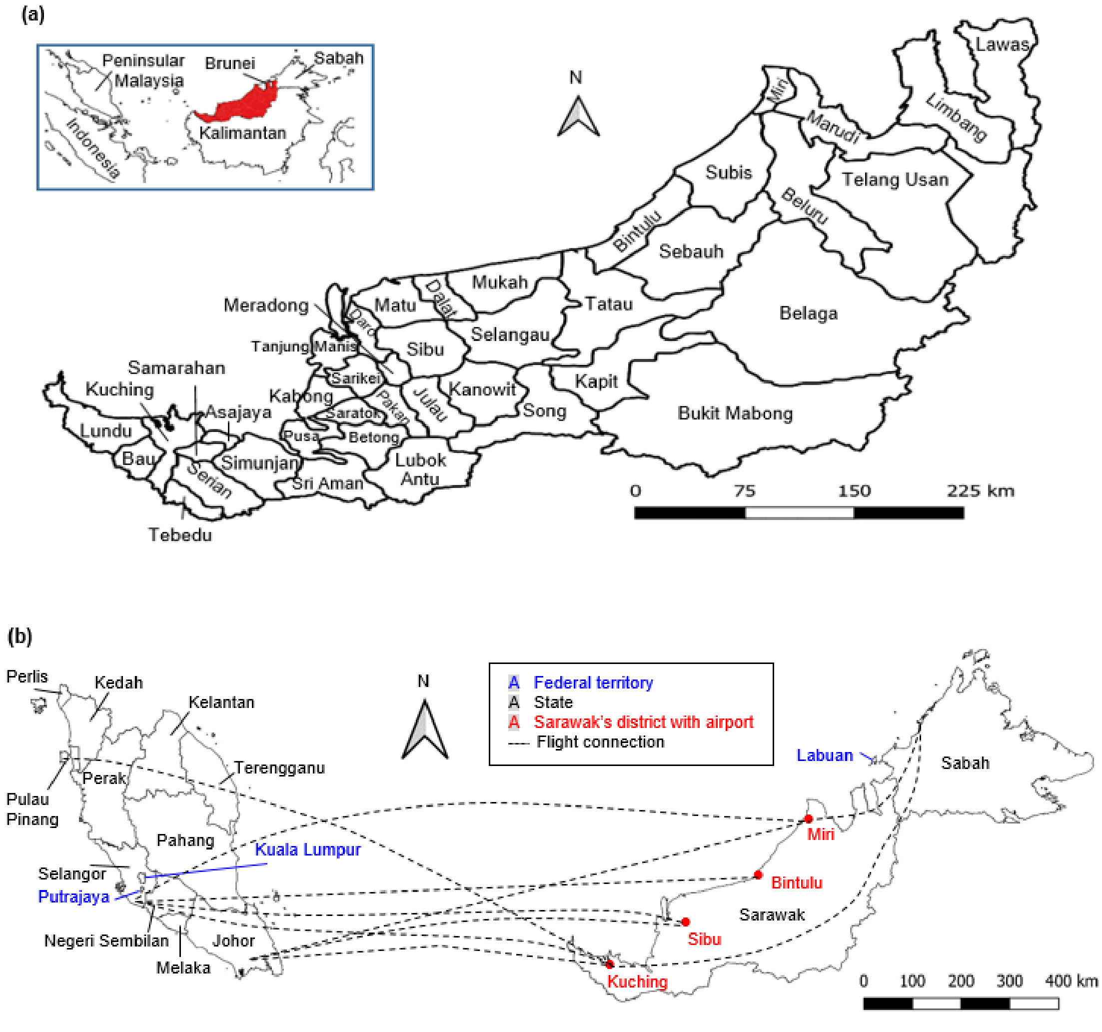

Figure 1. Geographical map of (a) 40 districts in Sarawak [25] (b) 13 states and three federal territories in Malaysia with flight connectivity considered in this study

As the largest state by land size in Malaysia and located in East Malaysia, Sarawak is geographically separated from Peninsular Malaysia by the South China Sea and can primarily be accessed from Peninsular by air transport. This unique geographical position may lead to the success of the state in controlling the disease transmission in year 2020 (see Fig. 2) while the country was placed under lockdown with severe restrictions on international and inter-state travel for a majority of months throughout the year. However, the spatiotemporal pattern of COVID-19 in Sarawak is strictly not a self-diffusion phenomenon that constrains solely within the state, but is highly related to the pandemic development outside the state. Transport networks such as flight connectivity or high-speed trains have been identified as playing a crucial role in the introduction and evolution of the COVID-19 outbreak worldwide in the early phase of the pandemic [30,31]. For instance, Krisztin and co-workers [32] considered the number of flight connections in their spatial econometric model and observed that the intensity of spatial spillover dropped due to travel restrictions. Hincapie and co-workers [33] found that the burden of illness was driven by case importation for the provinces with larger populations and greater connectivity. Despite the state of Sarawak's unique geographical characteristics, the spatial autocorrelation measure of the district-wise COVID-19 infection in the state must be investigated simultaneously with the incidence rates data in all 13 states and three federal territories of Malaysia. This can be accomplished by quantifying their spatial dependence through interaction-based adjacency matrix. Hence, this study also looked into the state-wise COVID-19 data which were publicly available on the GitHub page maintained by the Ministry of Health Malaysia.

2.2. Data Preprocessing

The Sarawak district-wise data throughout 2021 were first subdivided into four temporal periods using change point analysis algorithm. Change points are the points in time when abrupt variation in the statistical distributional properties of time series data is detected [34,35]. Many algorithms are available for detecting such change points in COVID-19 daily infection data (see, for instance [35,36]). Following our previous studies [25,37], we used a segment neighborhood technique in changepoint package in R [38] to split the daily cases data into a pre-defined four sub-segments whereby the data in each segment differ substantially in their statistical properties of both mean and variance. The state-wise data were segmented with the same temporal periods accordingly.

Since the state-level and Sarawak's district population sizes range approximately from 95 900 (Putrajaya) to 6 815 200 (Selangor), and from 7 900 (Tanjung Manis) to 609 200 (Kuching) respectively, in order to account for the difference in population sizes between states and districts, we calculated the COVID-19 incidence rates, either for a state or for a district, using (1).

$$\text{Incidence rate} = \frac{\begin{pmatrix}\text{The total number of daily confirmed cases in a} \\ \text{district (resp. state) within a temporal period}\end{pmatrix}}{\text{The population of the district (resp. state)}} \times 1000 \quad (1)$$

2.3. Spatial Weights

The spatial weights matrix (W) is a key element in spatial autocorrelation analysis. It is a non-diagonal square matrix of size $N \times N$, where N is the number of geographical units under observation. For contiguity-based spatial weights matrix, it has non-zero entries if two geographical units (say units i and j) share a common boundary, as defined by (2).

$$w_{ij} = \begin{cases} 1 & \text{if unit } j \text{ shares a common boundary} \\ & \text{with another unit } i \\ 0 & \text{otherwise} \end{cases} \quad (2)$$

The non-zero entries in spatial weights matrix indicate a spatial relationship is present between the two geographical units. Equation (2) only takes into account the immediate neighboring geographical units, therefore it is first-order contiguity matrix. Second-order contiguity can be specified by considering the neighbors of neighbor. The weights (w_{ij}) are then normalized for estimating the strength of spatial dependence between geographical units.

An example of first-order contiguity matrix for some selected states in Malaysia is illustrated in the top-left submatrix of Fig. 3. From Fig. 1(b), it can be seen that Selangor shares a common boundary with three other states (Negeri Sembilan, Pahang, and Perak) and two federal territories (Kuala Lumpur and Putrajaya). Hence, a normalized weight of 0.2 is assigned to the entries which pair Selangor to those states (or federal territories). However, such specification fails to describe the spatial dependence of Labuan, which is a small island situated off the coast of the state of Sabah. Therefore, a full weight of 1 is allocated to entry Labuan-Labuan so as to keep Labuan in our subsequent analysis. We denoted this state-level contiguity matrix as W_{ij}^{S}. The average number of links in this matrix is 2.56 with six states (or federal territories) having only one connected neighbor.

The spatial weights for Sarawak's districts were defined in a similar manner, which we denoted as W_{ij}^{D}. For instance, the entries for Subis are 0.25 (see the bottom-right submatrix in Fig. 3) as Subis shares boundary with four other districts (see Fig. 1(a)). The average number of links in this matrix is 4.4 with five districts having two contiguity neighbors while Sibu has the highest number of neighbors. The spatial weights are essential in calculating the variable known as spatial lag in spatial statistics. The spatial lag of the variable of interest, say the daily confirmed cases in a district, is the weighted average of all the district's neighbors' values. For instance, let's assume that Subis has zero daily confirmed cases on a particular day and its first-order contiguity neighbors, namely Beluru, Bintulu, Miri, and Sebauh have 4, 8, 4, and 12 daily cases respectively. Although Subis has zero daily cases, its spatial lag of daily cases is 6. Higher spatial lag value indicates greater chance of disease spillover from the neighboring districts. Hence, a precise definition of spatial weights is imperative in quantifying the spatial lag and studying the epidemic between different geographical units.

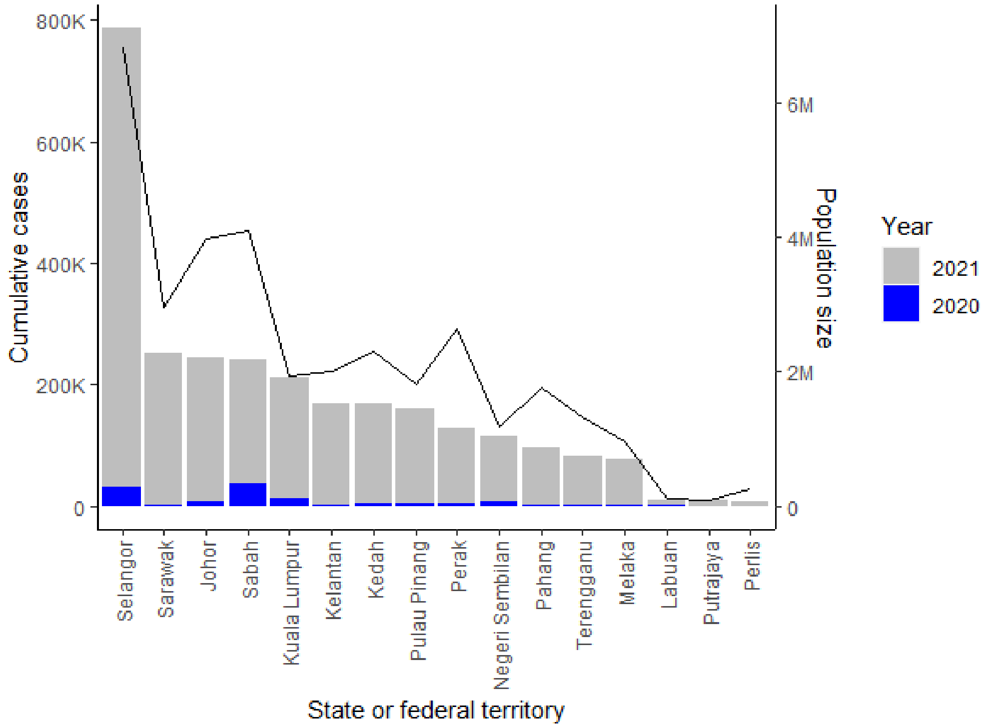

Figure 2. The bar plot of state-wise cumulative confirmed cases (in thousands) in Malaysia for years 2020 and 2021, as well as the line graph of the population size (in millions) of each state, which were obtained from the Department of Statistics Malaysia's website

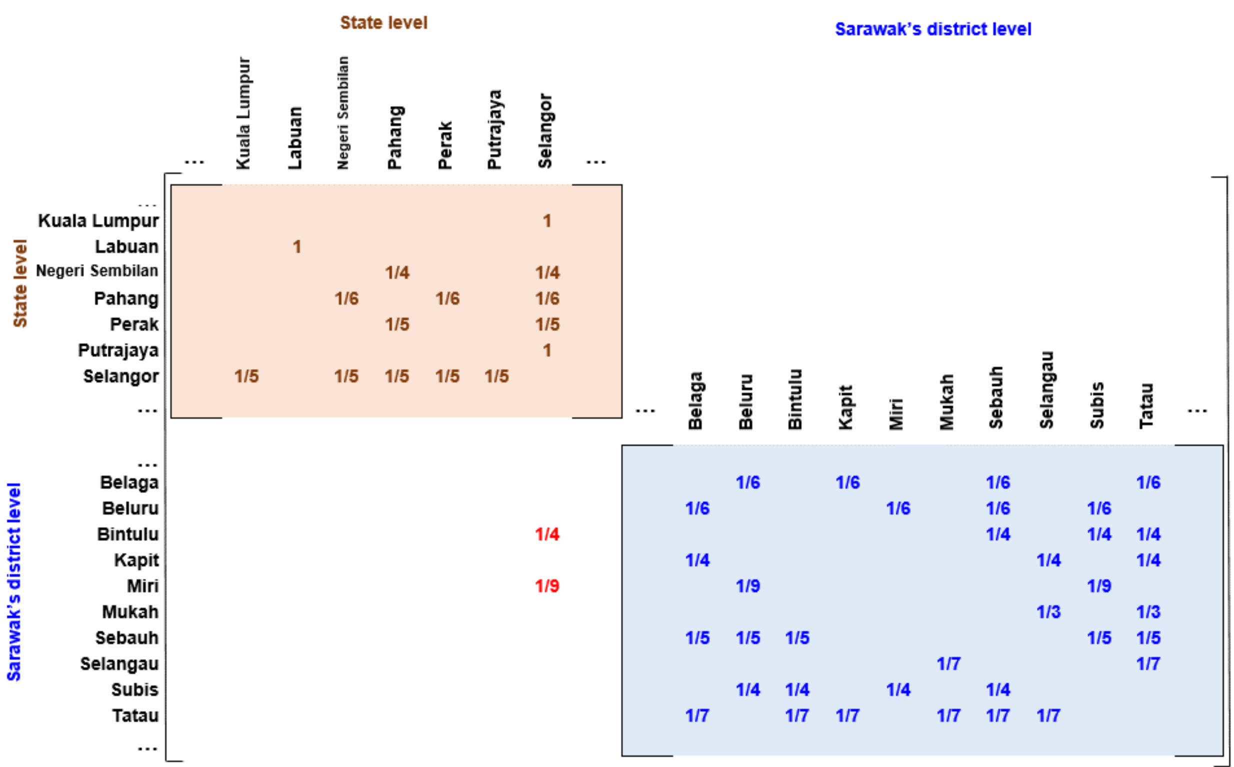

Figure 3. Schematic representation for part of the supra-adjacency spatial weights matrix

2.4. Supra-Adjacency Spatial Weights Matrix

A specific matrix structure is required when specifying the spatial weights for geographical units in more than one spatial aggregation level, such as the state and district levels in this study. In network science, the supra-adjacency matrix is commonly used for representing the intra- and inter-layer adjacency of a multi-layer network in one single large matrix, where the block diagonal submatrices constitute to the intra-layer adjacency and off-diagonal blocks quantify for the inter-layer connections. Borrowing this concept, we proposed a supra-adjacency spatial weights matrix to incorporate the intensity of spatial adjacency for two spatial aggregation levels for spatial statistics.

A schematic representation for part of the supra-adjacency matrix is given in Fig. 3. The spatial weights defined in the previous subsection indeed constitute to the intra-level adjacencies (denoted as W_{ij}^{SD}), which are depicted in brown color for state level and blue color for district level respectively in Fig. 3. We assume that COVID-19 transmission trajectories in Sarawak's districts are greatly influenced by the state-level disease propagation, but not vice versa. That is, the COVID-19 phenomena at the district level in Sarawak are solely affected by the pandemic situations at spatial aggregation level above it. Hence, we added inter-level spatial interactions for some selected economically developed and densely populated districts in Sarawak (namely Kuching, Sibu, Bintulu, and Miri) by considering their flight connectivity with other states in Malaysia (see Fig. 1(b)). These flight routes were selected as they have scheduled passenger service on commercial airlines between Sarawak and other states in Malaysia, even throughout the year 2021 in which SDMC imposed strict entry procedures for travelers entering Sarawak. Such assumptions and justifications, despite simplistic, may partially reflect the human mobility flow between other states and Sarawak.

An illustrative example of inter-level spatial interaction weights for the Bintulu district is highlighted in Fig. 3. In the first-order contiguity matrix, the weights assigned for the pair of Bintulu and its three neighboring districts, namely Sebauh, Subis, and Tatau, are supposed to be 1/3. However, as we assume COVID-19 situations in Bintulu are also greatly affected by situations in Selangor in which there is a direct flight route between Selangor and Bintulu, Bintulu will have an additional fourth neighbor (i.e. Selangor) at the state level. Therefore, the spatial lag of daily confirmed cases in Bintulu is the weighted average of all these four neighbors' values in supra-adjacency-based spatial weights specifications. The graphical description for the full supra-adjacency spatial weights matrix (denoted as $W_{ij}^{S \to D}$) is shown in Fig. 4. The summary of four different sets of spatial weights matrices used in this study is given in Table 1.

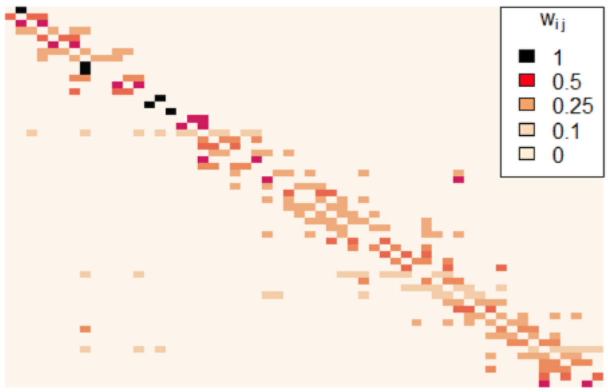

Figure 4. Graphical description of the supra-adjacency spatial weights matrix (of size 56 × 56) used in this study

2.5. Global and Local Spatial Autocorrelation Analysis

With the introduction of supra-adjacency-based spatial weights, it is possible to explore the spatial associations and clustering of COVID-19 incidence rates within Malaysia's states and Sarawak's districts, respectively. Most importantly, by incorporating inter-level adjacency in the supra-adjacency matrix, it allows for a nuanced investigation of the spatial autocorrelation measures of COVID-19 evolution in Sarawak under the influence of state-wise pandemic development.

Two types of spatial autocorrelation analysis were conducted. Global Moran's I statistic was first calculated to assess the significance of spatial clustering distribution patterns of the incidence rates at their spatial aggregation levels. This Moran's I statistic is indeed an extension of non-spatial Pearson correlation coefficient with spatial weights (w_{ij}) describing the spatial dependence among geographical units, as given by (3).

Table 1. Four sets of spatial weights matrices used in this study

No.	Geographical study area	Matrix size	Type of spatial weights	Matrix notation	Symbol
1	Sarawak's 40 districts	40 × 40	contiguity	W_{ij}^{D}	WD
2	Malaysia's 16 states	16 × 16	contiguity	W_{ij}^{S}	WS
3	Sarawak's 40 districts and Malaysia's 16 states	56 × 56	contiguity	W_{ij}^{SD}	WSD
4	Sarawak's 40 districts and Malaysia's 16 states; Flight connectivity	56 × 56	contiguity + interaction	$W_{ij}^{S \to D}$	WSA

Note: We use 'states' to refer to all 13 states and 3 federal territories in Malaysia.

$$I = \frac{N}{\sum_{i=1}^{N}\sum_{j=1}^{N} w_{ij}} \frac{\sum_{i=1}^{N}\sum_{j=1}^{N} w_{ij}(x_i-\bar{x})(x_j-\bar{x})}{\sum_{i=1}^{N}(x_i-\bar{x})^2}, \quad (3)$$

where x_i (resp. x_j) is the incidence rate at a particular (resp. another) geographical unit. The value of global Moran's I ranges from -1 (dispersed) to 1 (clustered), in which values close to zero indicate random spatial distribution and no spatial heterogeneity across the entire spatial domain.

Whenever global Moran's I is significant (i.e. p-value < 0.05), the exploration of local spatial autocorrelation can be performed to identify spatial clusters of high (hot spots) and low (cold spots) incidence rate patterns at the individual geographical units within the study area. Local Moran's I is expressed in (4) below.

$$I_i = \frac{(x_i-\bar{x})\sum_{j=1}^{N} w_{ij}(x_j-\bar{x})}{Var(x)} \quad (4)$$

The results of local spatial autocorrelation are commonly visualized in a cluster map known as local indicators of spatial association (LISA). Four types of clustering patterns exist, namely high-high, low-low, high-low, and low-high. In LISA map, the geographical units in high-high (resp. low-low) cluster are highlighted in red (resp. blue) whenever they have significant high (resp. low) incidence rates and have neighbors that also have high (resp. low) incidence rates. The other two spatial outlier clusters are colored in pink and pale blue for high-low and low-high associations respectively. Those geographical units identified as high-low cluster have high risk of spilling over disease to their neighboring units.

3. Results

3.1. Exploratory Spatial Data Analysis on Disease Incidence Rates

We first presented an overview of the COVID-19 incidence rates at Sarawak's district and Malaysia's state levels throughout the study period in Fig. 5. Although the state-level population sizes are predominantly larger than Sarawak's district level, their incidence rates (cases per 1 000 population) offset such differences. In the year of 2021, the Sarawak's districts COVID-19 incidence rates were not only generally higher than the state level's (see Fig. 5(a)), but also varied greatly within Sarawak. 10 out of 40 districts in Sarawak recorded higher than 120 cases per 1 000 population while the highest incidence rate at state level was Selangor with 110 cases. This may suggest that the spatial heterogeneity of the incidence rates at finer spatial aggregation level can be more substantial than those rates at coarser level.

We then illustrated the change point segmentation of Sarawak's daily confirmed cases data in Fig. 5(b). The blue horizontal lines denote the average number of daily cases over a specific temporal period. Note that the Wave 3 has an exceptional high average of 2 340 daily cases compared to just 509, 272, and 172 daily cases in Waves 2, 4, and 1 respectively. This indicates that the pandemic affected Sarawak most severely from August to October 2021 which is commonly regarded as Delta variant wave [39]. However, by superimposing the state-wise daily confirmed cases into the same figure, we found that this wave arrived in Sarawak two months later than in other states in Malaysia. This implies that different temporal periods of pandemic waves may be obtained if the change point segmentation is performed based on state-level data.

Based on the temporal periods obtained from the segmentation of Sarawak's data, the disease progression within Sarawak and across states in Malaysia for four temporal periods are depicted in Figs. 5(c) and 5(d) respectively. The outbreak began in the central region of Sarawak in early 2021, followed by higher incidence rates covering more districts in nearby regions in Wave 2 and gradually spread to all districts in Sarawak, with the most severe rates of incidence recorded in the southern region of Sarawak in Wave 3. At state level, higher incidence rates were observed from April to October 2021.

3.2. Global Spatial Autocorrelation Analysis

We gave the results of the global spatial autocorrelation analysis on the incidence rates for each spatial aggregation level throughout 2021 and across different waves in Table 2. The Moran's I statistics and their p-value for incidence rates in respective levels of Sarawak's districts and Malaysia's states were given first, followed by combining state and district levels using spatial contiguity matrix W_{ij}^{SD}, and lastly adding on top of that the spatial interaction submatrix $W_{ij}^{S\to D}$.

All the Moran's I statistics for Sarawak's district-level incidence rates are positive ranging from 0.21 to 0.37 and statistically significant (p-values < 0.05). The state-level incidence rates are found to have higher autocorrelation for Waves 1 and 2 with Moran's I of 0.59. However, the state-wise spatial autocorrelation is weaker than Sarawak's district level and not statistically significant for Wave 3, Wave 4, and throughout 2021. By combining both spatial dependence of Malaysia's states and Sarawak's districts in a purely spatial contiguity weights matrix (see the row of WSD in Table 2), the resulting Moran's I statistics are higher than those solely of the Sarawak's 40 districts over different temporal periods. The increases in the global spatial autocorrelation after including Malaysia states' incidence rates on top of the Sarawak 40 districts' may suggest the decreased variation in incidence rates between these regions, following the interpretation given in [40].

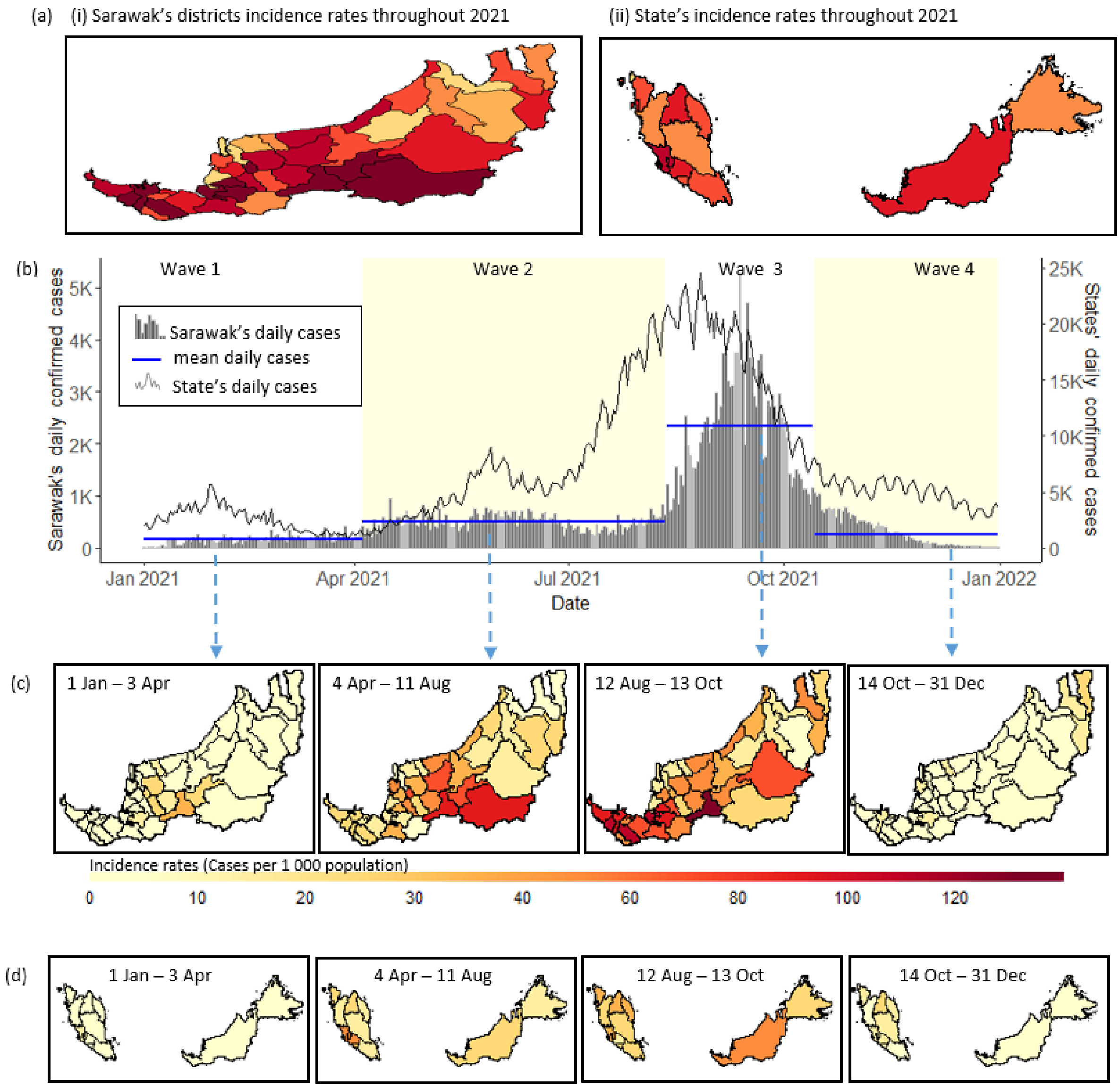

Figure 5. (a) The overall incidence rates throughout the study period for (i) Sarawak's districts and (ii) Malaysia's states. (b) The segmentation of study period into four temporal periods based on Sarawak's daily confirmed cases. The (c) Sarawak's districts' and (d) Malaysia's states' incidence rates in respective four temporal periods

Table 2. Global Moran's *I* statistics and their *p*-value of incidence rates for each spatial aggregation level throughout 2021 and across different waves

Spatial weights	Spatial level		Incidence rate				
			2021	Wave 1	Wave 2	Wave 3	Wave 4
WD	Sarawak's	Moran's *I*	0.213	0.214	0.373	0.329	0.277
	districts	*p*-value	0.022	0.021	1.28×10^{-4}	6.76×10^{-4}	0.003
WS	State	Moran's *I*	0.146	0.599	0.595	0.239	0.148
		p-value	0.358	0.004	0.004	0.188	0.188
WSD	State and	Moran's *I*	0.252	0.244	0.425	0.432	0.367
	district	*p*-value	0.009	0.011	1.89×10^{-5}	1.38×10^{-5}	1.96×10^{-4}
WSA	State and	Moran's *I*	0.249	0.246	0.426	0.413	0.371
	district	*p*-value	0.008	0.009	1.36×10^{-5}	2.34×10^{-5}	1.35×10^{-4}

When the flight connectivity is factored in a spatial interaction submatrix ($W_{ij}^{S \to D}$), the spatial autocorrelation intensities are altered differently over different waves, as shown in the row of WSA in Table 2. Specifically, for Waves 1 and 2 whereby the state-wise spatial autocorrelations are high and statistically significant, both the Sarawak district and Malaysia state incidence rates become slightly more spatially related. However, when the state-wise spatial autocorrelations are not statistically significant, both levels' Moran's I statistics drop marginally, except for Wave 4. As the Moran's I statistics are all moderate and statistically significant across different temporal periods, further exploration of their local clustering pattern through local spatial autocorrelation analysis is highly necessary.

3.3. Local Spatial Autocorrelation Analysis

We illustrated the local spatial autocorrelation through LISA cluster map in Fig. 6. By including the state-wise spatial autocorrelation through spatial contiguity weights W_{ij}^{SD} and spatial interaction submatrix $W_{ij}^{S \to D}$, several districts in Sarawak show contrasting results compared to the previous findings using first-order spatial contiguity weights in [25]. These districts were labelled in Fig. 6.

Overall, the LISA cluster maps in Fig. 6 agree considerably well with previous findings across different temporal periods, except for Wave 3 which gives greater deviation. In Wave 3 (see Fig. 6(d)), sporadic but significant low-high clusters are detected across three rural districts (Kabong, Pakan, and Bukit Mabong) in the central region of Sarawak. Also, a greater number of districts in the southern region fall into the high-high cluster. They include Bau, Lubok Antu, and Betong. All these districts, except Betong, were categorized as high-high cluster in the previous study only when the second-order contiguity weights were employed. This may suggest that incorporating spatial interaction with other states in Malaysia based on flight connectivity information in this study is able to capture more spatial clustering patterns of COVID-19 at the district level of Sarawak.

Sri Aman is one additional district grouped into high-high cluster for incidence rates throughout 2021 (Fig. 6(a)), while Sebauh is another new district with significant low-low clustering pattern in Wave 4 (Fig. 6(e)). Besides, Sibu district is now classified as high-high cluster in Wave 1 (Fig. 6(b)) with supra-adjacency spatial weights, which is otherwise detected only with the second-order contiguity weights in previous findings. This detection is remarkable especially because Sibu is highly related to the largest infection cluster in Sarawak known as Pasai Cluster, which represented the first widespread community transmission of COVID-19 infections in Sarawak. This infection cluster stemmed from an infected individual who returned from Johor to attend a funeral. This indicates that incorporating inter-level adjacency through spatial interaction submatrix may improve the spatial clustering detection effectiveness.

In Fig. 6, only subfigure 6(e) shows the map of Malaysia's states together with Sarawak's districts. This is because the state-level local spatial clustering pattern is only significant in Wave 4, but not for other temporal periods. Specifically, three adjacent states in the Peninsular Malaysia, namely Selangor, Pahang, and Terengganu, are categorized as high- high cluster while Perak is labelled as a significant low-high cluster in this wave. The detection of these three states as high-high cluster suggests that high local spatial autocorrelation may be responsible for the similar higher incidence rates around these adjacent states. No significant spatial clustering patterns were detected at the state-level incidence rates for the first nine months of 2021 mainly because the inter-state human flow remained low under the strict travel restrictions associated with Movement Control Order 2.0. When such travel restrictions were released in October 2021 [41], higher inter-state human flow gave rise to quicker spreading of virus transmission and therefore higher spatial clustering occurred.

3.4. Spatial Autocorrelation Analysis Based on the Segmentation of State-Level Data

In the previous subsections, we presented the spatial autocorrelation analysis of Malaysia's states and Sarawak's districts incidence rates over four temporal periods based on segmentation of Sarawak's daily confirmed cases. However, as can be seen from Fig. 5(b), such segmentation of periods may be different if the change point algorithm is applied to the state-wise daily confirmed cases. Specifically, the temporal segmentation and the way data are temporally aggregated are unavoidably susceptible to the modifiable temporal unit problem which has significant effects on the spatiotemporal incidence patterns and clusters detected [42,43]. Therefore, the consistencies of the spatial autocorrelation strength and local clustering pattern appearing at different temporal ranges need to be re-examined by considering different temporal segmentation of the datasets.

Hence, we performed the segmentation on the state data into four temporal segments using change point analysis and then subdivided the Sarawak's district data based on segmentation of state data. The date range of the resulting four temporal periods representing four pandemic waves at state level is given in Table 3. Waves 1, 3, and 4 are now covering longer period whereas Wave 2 becomes shorter if compared to the temporal segmentation shown in Fig. 5. Also, by inspecting their respective variance (results not given here), the incidence rates variability is found to be larger for these Waves 1, 3, and 4 whereas the opposite is observed for Wave 2. This may explain why the Moran's I statistics of incidence rates at state level are exceptional high (i.e. 0.839) during this Wave 2, as increased spatial autocorrelation may be caused by decreased variation in incidence across states when the time range of this Wave 2 is shorter.

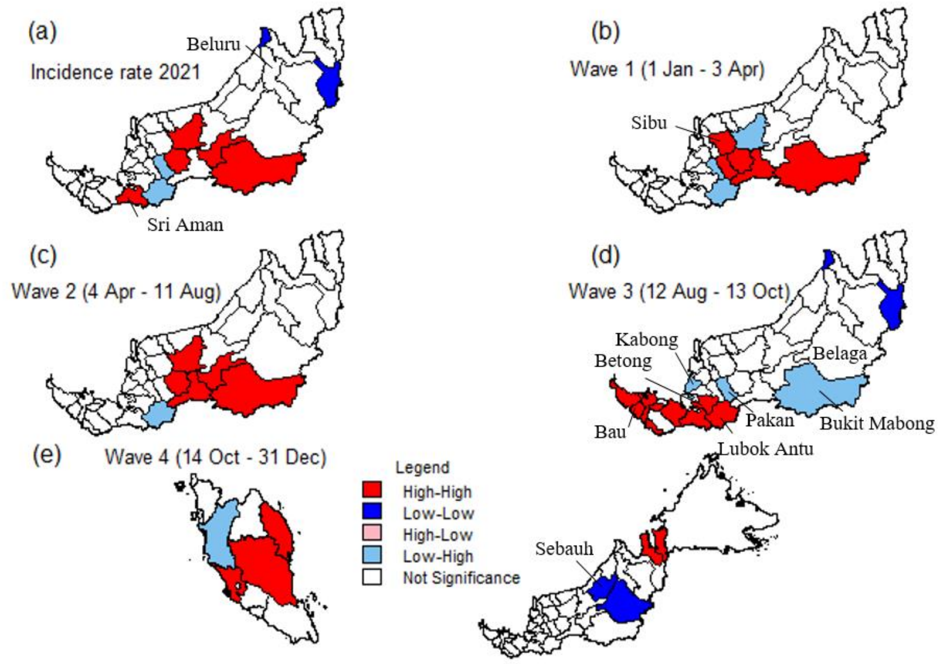

Figure 6. LISA cluster map for incidence rates in different temporal periods by using supra-adjacency spatial weights matrix

Table 3. Global Moran's *I* statistics and their *p*-value of incidence rates for different temporal periods segmented based on state-wise daily confirmed cases

Spatial weights	Spatial level		Incidence rate				
			2021	Wave 1 1 Jan – 16 May	Wave 2 17 May – 10 July	Wave 3 11 July – 8 Oct	Wave 4 9 Oct – 31 Dec
WD	Sarawak's districts	Moran's *I*	0.213	0.393	0.336	0.400	0.272
		p-value	0.022	5.87×10^{-5}	5.15×10^{-4}	4.41×10^{-5}	0.004
WS	State	Moran's *I*	0.146	0.403	0.839	0.222	0.146
		p-value	0.358	0.043	9.83×10^{-5}	0.214	0.359
WSD	State and district	Moran's *I*	0.252	0.434	0.521	0.421	0.283
		p-value	0.009	1.24×10^{-5}	2.01×10^{-7}	2.18×10^{-5}	3.61×10^{-3}
WSA	State and district	Moran's *I*	0.249	0.432	0.520	0.402	0.284
		p-value	0.008	1.03×10^{-5}	1.35×10^{-7}	3.83×10^{-5}	2.99×10^{-3}

Overall, the statistical significances of the global Moran's *I* in Table 3 across different spatial aggregation levels remain consistent with results given in Table 2. For instance, similar to Table 2, all global Moran's *I* statistics for four temporal periods in Table 3 are significant (p-value < 0.05) except the state-level incidence rates in Waves 3 and 4. From the row of WSA, the inclusion of spatial interaction submatrix results in weakening the global spatial autocorrelation (i.e. a lower global Moran's *I*) over the first three waves. A slightly smaller global Moran's *I* value may suggest a more dispersed spatial distribution of incidence rates. This is particular true where the spatial interaction submatrix can be regarded as partially representing the human flow between selected Malaysia's states and Sarawak's districts through flight connectivity.

We then illustrated the local clustering pattern of incidence rates for different temporal periods segmented based on the state-wise data in the form of LISA maps in Fig. 7. Despite different temporal segmentation, the LISA maps in Fig. 7 are almost identical to those in Fig. 6 for Waves 2 and 4, except that Julau is categorized as low-high in Wave 2 and no significant local clusters are detected at state level in Wave 4. The latter may suggest that the segmentation of the data alters the local clustering results at state level more considerably compared to Sarawak's district level. As Wave 1 spans longer period, three additional districts, namely Selangau, Pakan, and Kapit, are detected as high-high (see Fig. 7(b)). Serian is a newly found high-high cluster while Lubok Antu is in low-low in Wave 3 (see Fig. 7(d)). The consistency of the other not specially mentioned clusters in Fig. 7 (and Fig. 6) suggests that these clusters can be considered as 'true' clusters which are stronger than the others [42].

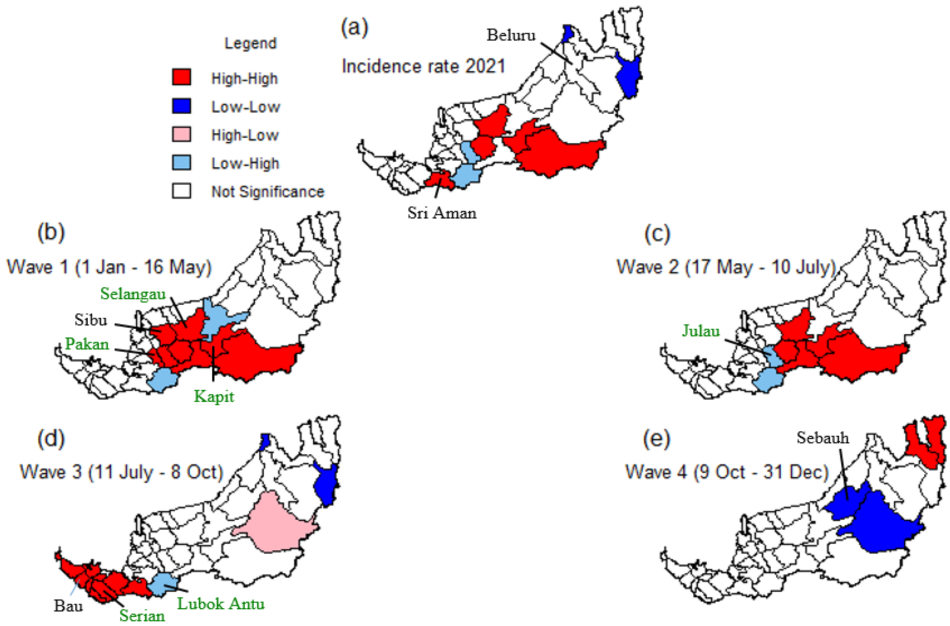

Figure 7. LISA cluster map for incidence rates in different temporal periods segmented based on state-wise daily confirmed cases. The additional significant clusters found in this LISA compared to those in Fig. 6 are indicated with green label

4. Discussion

This study utilized a novel supra-adjacency-based spatial weights matrix to explore the global and local spatial autocorrelation strength of pandemic evolution across 40 districts in Sarawak in conjunction with the disease development at state level of Malaysia over different temporal periods. The spatial linkage structure between these districts and states was implicitly modelled as inter-layer adjacency by considering the flight routes between four districts in Sarawak and several other states in Malaysia. Segmentation of data based on Sarawak's and state-wise daily confirmed cases data was conducted. Together with the supra-adjacency weights matrix, the consistency of the intensity of spatial autocorrelation and type of local clustering patterns at two spatial aggregation levels over time were investigated.

The detection of Sibu as an additional high-high cluster in Wave 1 (see Fig. 6(b)) in this supra-adjacency weights matrix is remarkable. Although Sibu has the highest number of first-order contiguity neighbors among all 40 districts in Sarawak, it is still not categorized as significant high-high cluster under the purely first-order spatial contiguity weights scheme in the previous study [25]. As a district with large number of spatial contiguity neighbors, the spatial lag of the disease incidence rate in Sibu can be offset by smaller incidence rates in its adjacent rural districts such as Daro and Matu. When the spatial interaction between Sibu and Johor (resp. Selangor) is added through submatrix $W_{ij}^{S\rightarrow D}$ in supra-adjacency setting, these states' incidence rates greatly impact the spatial lag of the disease incidence rates in Sibu. The inclusion of Johor as a neighbor to Sibu is highly relevant since the start of widespread community outbreak of COVID-19 in the center of Sarawak was linked to Pasai infection cluster. This infection cluster was associated with inter-state travel from Johor due to funerals [44]. Sibu district not only serves as the geographic center of Sibu division and Sarawak, but also offers a highly convenient facility for handling COVID-19 testing and case registration [45] for its nearby districts. These suggested that Sibu's incidence rate had a profound effect on the emergence of Wave 1 in Sarawak and indicated the need to include Sibu as a high-high cluster in this temporal period.

When spatial autocorrelation analysis is performed across different aggregations of incidence data, namely aggregation by district for Sarawak state, and aggregation by state for all 13 states and three federal territories in Malaysia, the potential data quality issues caused by different levels of spatial aggregation of data can be revealed. Although the global Moran's I is generally higher for incidence rates in state level than in district level during Waves 1 and 2 (see Tables 2 and 3), the local clustering patterns at this coarser level of aggregation may be faded out. Specifically, the LISA cluster maps in Figs. 6 and 7 indicate that the numbers of significant spatial clusters and outliers in district level are substantially greater than its state-level counterpart. Only four states in Wave 4 appear to form significant cluster (see Fig. 6(e)). This suggests that aggregation at coarse-grained levels fail to keep valuable attribute and may underestimate the severity of the virus spread in the course of pandemic [46]. However, such aggregation is essentially a tradeoff between the level of detail and noise in spatial analysis [47]. Coarser level implies fewer regions are being analyzed. Although this may reduce detail information, extreme values in the data can be conveniently averaged out. Hence, public health researchers should treat the aggregated data at coarse-grained levels with greater caution.

Previous studies have reported that the COVID-19 transmission in a state not only occurs in adjoining counties, but also spills among different states which are geographically distant from the source state [48,49]. Therefore, the spatial contiguity alone might not be sufficient for comprehending the COVID-19 diffusion due to human interactions, given the modern transportation facilities and socioeconomic dependencies between regions [23]. Hence, several domestic flight routes (see Fig. 1(b)) were considered in this study for incorporating the spatial interaction effect on the disease incidence rates between states in Malaysia and districts in Sarawak. We assume the source states are those outside Sarawak. That is, the disease spills over from those states to Sarawak through positioning the submatrix $W_{ij}^{S\to D}$ at bottom left of the supra-adjacency matrix (see Figs. 3 and 4). It is mathematically plausible to add another submatrix $W_{ij}^{D\to S}$ at the top-right of the supra-adjacency matrix and assume that the disease may also spill over from Sarawak to other states in Malaysia. We opted for not implementing this partially because it was evidence from the Fig. 5(b) that the state-wise pandemic waves arrived earlier than those in district level of Sarawak.

4.1. Public Health Implications, limitations and Future Directions

The supra-adjacency matrix approach has significant practical applications for public health decision-making and pandemic preparedness. Capturing inter-layer spatial dependencies allows for more targeted interventions, such as optimizing vaccine distribution and planning mobility restrictions during pandemics. This methodology can strengthen early warning systems by identifying high-risk clusters often overlooked by traditional spatial models. Studies have emphasized addressing spatial uncertainties to improve epidemiological predictions [50] and the value of hybrid spatial weights in detecting high-risk areas [51]. Furthermore, its scalability aligns with global efforts to enhance disease surveillance, as highlighted in multiscale network modelling studies [50,52].

This study has several limitations. First, the study period was limited to one year (i.e. 2021). Both the Sarawak's district level incidence data for the first year of the pandemic and for the omicron wave in the third year were not publicly available. However, since the COVID-19 cases in Sarawak were relatively small in the year 2020, and the relaxation of flight frequencies into Sarawak started before the arrival of the omicron wave, the spatial autocorrelation we observed is consistent across different segmentation of temporal periods throughout the year 2021. Second, we have no way to adjust the spatial interaction weights between states in Malaysia and districts in Sarawak based on the actual interstate travel across different temporal periods in 2021. Such human mobility flow data are scarce for the developing state like Sarawak. Even so, this adjustment may be deemed necessary as the whole country including Sarawak imposed different intensity of travel restrictions as non-pharmaceutical interventions across different months of 2021. Spatial dependence greatly decreased when lockdown was implemented [32].

Future research should focus on incorporating real-world mobility data, refining temporal segmentation, integrating socio-economic factors, and ensuring scalability. Human mobility data can enhance spatial interaction matrices by reflecting actual movement patterns [53,54]. Addressing spatiotemporal uncertainties is also critical for capturing variations in disease dynamics across different regions and timeframes [50]. Additionally, incorporating socio-economic data, such as population density and healthcare accessibility, could refine spatial weights and improve cluster detection [51]. Finally, scaling these methods to larger and more complex networks, such as global air transport systems, would allow broader applicability in monitoring cross-border disease transmission [50,52].

5. Conclusions

We have provided evidence that the spatial dependencies of COVID-19 incidence rates at two different aggregation levels and concerning geographical disjoint regions can be conceptualized using supra-adjacency weights matrix. Such weights matrix incorporates spatial interaction into spatial contiguity for quantifying inter-level adjacency. Assessing such adjacency of the inter- and intra-level spread of COVID-19 could provide valuable insight into understanding the observed spatial autocorrelation patterns across multiple spatial scales. This is crucial for optimizing medical resources and public health interventions decision-making. The methodology and its subsequent results analysis can serve as a reference for disease surveillance and response in preparation for next pandemic or more generally epidemic diseases outbreaks.

Acknowledgements

This research was conducted with publicly available data published by Ministry of Health Malaysia and Sarawak Disaster Management Committee. The authors would like to thank Universiti Malaysia Sarawak for providing the Zamalah Scholarship to Saira Aslam, computing facilities, and partial publication funding.

REFERENCES

[1] Franch-Pardo I., Napoletano B.M., Rosete-Verges F., Billa L. "Spatial analysis and GIS in the study of COVID-19. A

review," Science of the Total Environment, 739, 140033, 2020. https://doi.org/10.1016/j.scitotenv.2020.140033

[2] Ahasan R., Alam M.S., Chakraborty T., Hossain M.M. "Applications of GIS and geospatial analyses in COVID-19 research: A systematic review." F1000Research, 9, 2020. https://doi.org/10.12688/f1000research.27544.2

[3] N. Nazia, Butt Z.A., Bedard M.L., Tang W.C., Sehar H., Law J. "Methods used in the spatial and spatiotemporal analysis of COVID-19 epidemiology: a systematic review," International Journal of Environmental Research and Public Health, 19(14), 8267, 2022. https://doi.org/10.3390/ijerph19148267

[4] Saran S., Singh P., Kumar V., Chauhan P. "Review of geospatial technology for infectious disease surveillance: Use case on COVID-19," Journal of the Indian Society of Remote Sensing, 48, 1121-1138, 2020. https://doi.org/10.1007/s12524-020-01140-5

[5] Kianfar N., Mesgari M.S. "GIS-based spatio-temporal analysis and modeling of COVID-19 incidence rates in Europe," Spatial and Spatio-temporal Epidemiology, 41, 100498, 2022. https://doi.org/10.1016/j.sste.2022.100498

[6] Kang D., Choi H., Kim J.H., Choi J. "Spatial epidemic dynamics of the COVID-19 outbreak in China," International Journal of Infectious Diseases, 94, 96-102, 2020. https://doi.org/10.1016/j.ijid.2020.03.076

[7] Dutta I., Basu T., Das. A. "Spatial analysis of COVID-19 incidence and its determinants using spatial modeling: A study on India," Environmental Challenges, 4, 100096, 2021. https://doi.org/10.1016/j.envc.2021.100096

[8] Reveshty M.A., Heydari M.T., Tahmasebimoghaddam H. "Spatial analysis of the factors impacting on the spread of Covid-19 in the neighborhoods of Zanjan, Iran," Spatial Information Research, 32(2), 151-164, 2024. https://doi.org/10.1007/s41324-023-00550-0

[9] Olu O.T. et al. "Propagation dynamics of meningitis disease based on complex network modeling," Universal Journal of Public Health, 11(3), 324-331, 2023. https://doi.org/10.13189/ujph.2023.110306

[10] Affandi P., Ahsar M.K, Suhartono E., Dalle J. "Systematic review: mathematics model epidemiology of dengue fever. Universal Journal of Public Health, 10(4), 419-429, 2022. https://doi.org/10.13189/ujph.2022.100415

[11] Getis A. "A history of the concept of spatial autocorrelation: A geographer's perspective," Geographical Analysis, 40(3), 297-309, 2008. https://doi.org/10.1111/j.1538-4632.2008.00727.x

[12] Bavaud F. "Models for spatial weights: a systematic look," Geographical Analysis, 30(2), 153-171, 1998. https://doi.org/10.1111/j.1538-4632.1998.tb00394.x

[13] Zhang X., Yu Y. "Spatial weights matrix selection and model averaging for spatial autoregressive models," Journal of Econometrics, 203(1), 1-18, 2018. https://doi.org/10.1016/j.jeconom.2017.05.021

[14] Potgieter A., Fabris-Rotelli I.N., Kimmie Z., Dudeni-Tlhone N., Holloway J.P., Janse van Rensburg C., Khuluse-Makhanya, S. "Modelling representative population mobility for COVID-19 spatial transmission in South Africa," Frontiers in Big Data, 4, 718351, 2021. https://doi.org/10.3389/fdata.2021.718351

[15] Sarkar S.K., Ekram K.M.M., Das P.C. "Spatial modeling of COVID-19 transmission in Bangladesh," Spatial Information Research 1-12, 2021. https://doi.org/10.1007/s41324-021-00387-5

[16] Kang D., Choi J., Kim Y., Kwon D. "An analysis of the dynamic spatial spread of COVID-19 across South Korea," Scientific Reports, 12(1), 9364, 2022. https://doi.org/10.1038/s41598-022-13301-2

[17] Perret J.K. "A proposal for an alternative spatial weight matrix under consideration of the distribution of economic activity," 2011-002, Schumpeter Discussion Papers, 2011.

[18] Janatabadi F., Ermagun A. "Access weight matrix: A place and mobility infused spatial weight matrix," Geographical Analysis, 56, 746-767, 2024. https://doi.org/10.1111/gean.12395

[19] Ejigu B.A., Wencheko E. "Introducing covariate dependent weighting matrices in fitting autoregressive models and measuring spatio-environmental autocorrelation," Spatial Statistics, 38, 100454, 2020. https://doi.org/10.1016/j.spasta.2020.100454

[20] Fotheringham A.S., O'Kelly M.E. "Spatial interaction models: Formulations and applications," 1, pp. 989, Dordrecht: Kluwer Academic Publishers, 1989.

[21] Briz-Redon A., Iftimi A., Correcher J.F., De Andrés J., Lozano M., Romero-García C. "A comparison of multiple neighborhood matrix specifications for spatio-temporal model fitting: a case study on COVID-19 data," Stochastic Environmental Research and Risk Assessment, 36(1), 271-282, 2022. https://doi.org/10.1007/s00477-021-02077-y

[22] Dong K., Guo L. "Research on the spatial correlation and spatial lag of COVID-19 infection based on spatial analysis," Sustainability, 13(21), 12013, 2021. https://doi.org/10.3390/su132112013

[23] Belvis F., Aleta A., Padilla-Pozo Á., Pericàs J.M., Fernández-Gracia J., Rodríguez J.P., Eguiluz V.M., De Santana C.N., Julia M., Benach J., the COVID-SHINE group. "Key epidemiological indicators and spatial autocorrelation patterns across five waves of COVID-19 in Catalonia," Scientific Reports, 13(1), 9709, 2023. https://doi.org/10.1038/s41598-023-36169-2

[24] Cheong Y.L., Ghazali S.M., Che Ibrahim M.K.B., Kee C.C., Md Iderus N.H., Ruslan Q.B., Lim, K.H. "Assessing the spatiotemporal spread pattern of the COVID-19 pandemic in Malaysia," Frontiers in Public Health, 10, 836358, 2022. https://doi.org/10.3389/fpubh.2022.836358

[25] Phang P., Labadin J., Suhaila J., Aslam S., Hazmi H. "Exploration of spatiotemporal heterogeneity and socio-demographic determinants on COVID-19 incidence rates in Sarawak, Malaysia," BMC Public Health, 23(1), 1396, 2023. https://doi.org/10.1186/s12889-023-16300-8

[26] Chaudhuri S., Srivastava A. "Network approach to understand biological systems: From single to multilayer networks," Journal of Biosciences, 47(4), 55, 2022. https://doi.org/10.1007/s12038-022-00285-4

[27] Kivelä M., Arenas A., Barthelemy M., Gleeson J. P., Moreno Y., Porter M.A. "Multilayer networks," Journal of

Complex Networks, 2(3), 203-271, 2014.https://doi.org/10.1093/comnet/cnu016

[28] Westernhagen C.H., Bagheri A., Garcia-Bernardo J. “Predicting COVID-19 infections using multi-layer centrality measures in population-scale networks,” Applied Network Science, 9(1), 27, 2024. https://doi.org/10.1007/s41109-024-00632-4

[29] Phang P., Yap M.Y., Zakaria S., Labadin J. “Geo-visualization of Sarawak COVID-19 Publicly Available Data Employing Open-source Geospatial Software,” Universal Journal of Public Health, 11, 34-49, 2023. https://doi.org/10.13189/ujph.2023.110105

[30] Sun X., Wandelt S., Zhang A. “On the degree of synchronization between air transport connectivity and COVID-19 cases at worldwide level,” Transport Policy 105, 115-123, 2021. https://doi.org/10.1016/j.tranpol.2021.03.005

[31] Su M., Hu B., Jiang Y., Zhang Z., Li Z. “Relationship between the Chinese main air transport network and COVID-19 pandemic transmission,” Mathematics, 10(13), 2348, 2022. https://doi.org/10.3390/math10132348

[32] Krisztin T., Piribauer P., Wögerer M. “The spatial econometrics of the coronavirus pandemic,” Letters in Spatial and Resource Sciences, 13, 209-218, 2020. https://doi.org/10.1007/s12076-020-00254-1

[33] Hincapie R., Munoz D.A., Ortega N., Isfeld-Kiely H.K., Shaw S.Y., Keynan Y., Rueda Z.V. “Effect of flight connectivity on the introduction and evolution of the COVID-19 outbreak in Canadian provinces and territories,” Journal of Travel Medicine, 29(8), taac100, 2022. https://doi.org/10.1093/jtm/taac100

[34] Aminikhanghahi S., Cook D.J. “A survey of methods for time series change point detection,” Knowledge and Information Systems, 51(2), 339-367, 2017. https://doi.org/10.1007/s10115-016-0987-z.

[35] Gargoum S.A. Gargoum A.S. “Limiting mobility during COVID-19, when and to what level? An international comparative study using change point analysis,” Journal of Transport & Health, 20, 101019, 2021. https://doi.org/10.1016/j.jth.2021.101019

[36] Jegede S.L. Szajowski K.J. “Change-point detection in homogeneous segments of COVID-19 daily infection,” Axioms, 11(5), 213, 2022. https://doi.org/10.3390/axioms11050213

[37] Phang P., Taib N.A., Safii R., Labadin J. “Piecewise linear modelling and change-point analysis of COVID-19 outbreak in Malaysia,” Journal of Physics: Conference Series, 1988(1), 012105, 2021. https://doi.org/10.1088/1742-6596/1988/1/012105

[38] Killick R., Eckley I.A. “changepoint: An R package for changepoint analysis,” Journal of Statistical Software 58, 1-19, 2014.

[39] Md Iderus N.H., Lakha Singh S.S., Mohd Ghazali S., Cheong Y.L., Tan C.V., Md Zamri A.S.S., Ahmad Jaafar N., Ruslan Q., Ahmad Jaghar N.H., Gill B.S. “Correlation between population density and COVID-19 cases during the third wave in Malaysia: Effect of the delta variant,” International Journal of Environmental Research and Public Health 19(12), 7439, 2022. https://doi.org/10.3390/ijerph19127439

[40] Souty C., Turbelin C., Blanchon T., Hanslik T., Le Strat Y., Boëlle P.Y. “Improving disease incidence estimates in primary care surveillance systems,” Population Health Metrics, 12, 1-9, 2014. https://doi.org/10.1186/s12963-014-0019-8

[41] Tang K.H.D. “From movement control to national recovery plan: Malaysia’s strategy to live with COVID-19,” International Journal of Science and Healthcare Research, 6(4), 286-292, 2021.

[42] Cheng T., Adepeju M. “Modifiable temporal unit problem (MTUP) and its effect on space-time cluster detection,” PloS One, 9(6), e100465, 2014. https://doi.org/10.1371/journal.pone.0100465

[43] Helbich M., Browning M.H.M., Kwan M.P. “Time to address the spatiotemporal uncertainties in COVID-19 research: Concerns and challenges,” Science of the Total Environment, 764, 142866, 2021. https://doi.org/10.1016/j.scitotenv.2020.142866

[44] Liau J., Ahmad S.S.W., Ishak S.Z.A. “Covid-19, Mortality and Inequality in Sarawak,” Journal of Borneo-Kalimantan 9, 2, 2023.

[45] Jeta D., Azmi A. “Spatial and Temporal Analysis of Covid-19 in Sibu, Sarawak,” Malaysian Journal of Medicine & Health Sciences, 19, 2023.

[46] Cheng Y.Y., Ludäscher B. “Through the magnifying glass: Exploring aggregations of COVID-19 datasets by county, state, and taxonomies of US regions,” Proceedings of the Association for Information Science and Technology, 57(1), e355, 2020. https://doi.org/10.1002/pra2.355

[47] Oshan T.M., WolF L.J., Sachdeva M., Bardin S., Fotheringham A.S. “A scoping review on the multiplicity of scale in spatial analysis,” Journal of Geographical Systems, 24(3), 293-324, 2022. https://doi.org/10.1007/s10109-022-00384-8

[48] Liu L., Hu T., Bao S., Wu H., Peng Z., Wang R. “The spatiotemporal interaction effect of COVID-19 transmission in the United States,” ISPRS International Journal of Geo-Information, 10(6), 387, 2021. https://doi.org/10.3390/ijgi10060387

[49] Zhang C., Zhang D. “Spatial interactions and the spread of covid-19: a network perspective,” Computational Economics, 62(1), 383-405, 2023. https://doi.org/10.1007/s10614-022-10278-y

[50] Huang J., Kwan M.P. “Uncertainties in the assessment of COVID-19 risk: A study of people’s exposure to high-risk environments using individual-level activity data,” Annals of the American Association of Geographers, 112(4), 968-987, 2022. https://doi.org/10.1080/24694452.2021.1943301

[51] Silva M., Viana C.M., Betco I., Nogueira P., Roquette R., Rocha J. “Spatiotemporal dynamics of epidemiology diseases: mobility based risk and short-term prediction modeling of COVID-19,” Frontiers in Public Health, 12, 1359167, 2024. https://doi.org/10.3389/fpubh.2024.1359167

[52] Byun H.G., Lee N., Hwang S.S. “A systematic review of spatial and spatio-temporal analyses in public health

research in Korea," Journal of Preventive Medicine and Public Health, 54(5), 301-308, 2021. https://doi.org/10.3961/jpmph.21.160

[53] Kostandova N., Schluth C., Arambepola R., Atuhaire F., Bérubé S., Chin T., Wesolowski A. "A systematic review of using population-level human mobility data to understand SARS-CoV-2 transmission," Nature Communications, 15(1), 1-12, 2024. https://doi.org/10.1038/s41467-024- 54895-7

[54] Li H., Huang J., Lian X., Zhao Y., Yan W., Zhang L., Li L. "Impact of human mobility on the epidemic spread during holidays," Infectious Disease Modelling, 8(4), 1108-1116, 2023. https://doi.org/10.1016/j.idm.2023.10.001